

# Structural study of a $\text{Ag}_{3.4}\text{In}_{3.7}\text{Sb}_{76.4}\text{Te}_{16.5}$ quadruple compound utilized for phase-change optical disks

Toshiyuki Matsunaga,<sup>1,\*</sup> Yukihiro Umetani,<sup>1</sup> and Noboru Yamada<sup>2</sup><sup>1</sup>Characterization Technology Group, Matsushita Technoresearch, Inc., 3-1-1 Yagumo-Nakamachi, Moriguchi, Osaka 570-8501, Japan<sup>2</sup>Optical Disk Systems Development Center, Matsushita Electric Industrial Co., Ltd., 3-1-1 Yagumo-Nakamachi, Moriguchi, Osaka 570-8501, Japan

(Received 15 May 2001; revised manuscript received 8 August 2001; published 25 October 2001)

The behavior of a quadruple compound,  $\text{Ag}_{3.4}\text{In}_{3.7}\text{Sb}_{76.4}\text{Te}_{16.5}$ , is investigated at various temperatures using the large Debye-Scherrer camera installed in BL02B2 at SPring-8, to elucidate its crystal structure. The low-temperature phase of this crystal has an  $A7$  structure with atoms of Ag, In, Sb, or Te randomly occupying the  $6(c)$  site in the  $R\bar{3}m$  space group. The crystal lattice thermally expands almost linearly with increasing temperature between 81 K and around 850 K. The crystal structure shows little change between 81 K and around 600 K however, above 600 K, marked changes with increased temperature are observed with respect to the thermal vibration of atoms, interatomic distances and bond angles. The  $A7$  structure transforms at approximately 780 K to a rhombohedral structure that includes only one atom in each unit cell. This change of structure is thought to be a second-order phase transition. The compound  $\text{Ag}_{3.4}\text{In}_{3.7}\text{Sb}_{76.4}\text{Te}_{16.5}$  can maintain its crystalline phase up to approximately 850 K, but at higher temperatures it changes into an amorphous phase.

DOI: 10.1103/PhysRevB.64.184116

PACS number(s): 61.10.Nz

## I. INTRODUCTION

A thin film of AgInSbTe-based compounds is used as the memory layer in phase-change type optical disk media. Recording can be achieved by irradiating a laser beam onto a thin film of this compound to cause reversible phase changes between the amorphous and crystalline phases, and by optically detecting the changed state, for example as different reflectivity. The crystal structure of a photorecording material has a strong influence on its optical characteristics, cycle characteristics and record-erase characteristics.<sup>1</sup> Thus, identifying a compound's crystal structure is a prerequisite for improving its performance as a recording medium. Very little research, however, has been carried out on the crystal structure of this material. The primary reason for this is that the diffraction lines obtained by means of conventional x-ray diffractometers used in laboratories show a significant overlapping of the peaks as shown in Fig. 1, impeding clear identification of the crystal structure. In order to solve the angular resolution problem, powder diffraction data were collected by using a large-diameter Debye-Scherrer camera and well-monochromated synchrotron radiation. The Debye-Scherrer camera allows the simultaneous collection of multiple diffraction lines. In contrast to the line spectrum generated by an x-ray tube, the synchrotron radiation spectrum is smooth over a large range of energies. This makes it possible to choose the wavelength best suited to the experimental problem in question. Moreover, synchrotron radiation facilities generate intense x-rays, making it possible to collect precise x-ray-diffraction data within a reasonably short time. In this paper, we describe and discuss the results of crystallographical research on an AgInSbTe-based compound carried out using a Debye-Scherrer camera and synchrotron radiation.

## II. EXPERIMENT

A thin film of  $\text{Ag}_{3.4}\text{In}_{3.7}\text{Sb}_{76.4}\text{Te}_{16.5}$  with a thickness of approximately 5000 Å was formed by sputtering on a glass

disk 120 mm in diameter. The film was crystallized by means of laser irradiation and was then scraped off with a spatula to create a powder. To prepare the experimental specimen for x-ray diffraction, the powder was then packed into a quartz capillary tube with an internal diameter of 0.2 mm. Both ends of the capillary were open to the air. The diffraction experiments were carried out using the large-diameter Debye-Scherrer camera with an imaging plate on the BL02B2 beam line at the Japan Synchrotron Radiation Research Institute (SPring-8).<sup>2,3</sup> A precollimator mirror and a double-crystal spectrometer were used to ensure that the incident beam used for the diffraction experiments was extremely monochromatic and parallel. The camera radius was 278 mm and the pixel area of the imaging plate was  $100 \mu\text{m}^2$ , corresponding to an angular resolution of approximately  $0.02^\circ$ . To enable a precise structure analysis, it is important for each diffraction peak to be comprised of sufficient data points. Measurements at a low temperature (81 K) and at room temperature (300 K) were made using a single 40-min exposure followed by a second exposure after shifting the  $2\theta$  axis by  $0.01^\circ$ . The combination of the two measurements is equivalent to data with a step width of  $0.01^\circ$ . In order to confirm the radiation beam energy used, diffraction pattern of powdered  $\text{CeO}_2$  ( $a = 5.4111 \text{ \AA}$ ) was taken under the same condition. Experiments at low and high temperature were carried out while blowing nitrogen gas set at the specified temperatures onto the capillary tube. The high-temperature experiments were carried out by collecting diffraction data with an angular resolution of  $0.02^\circ$  while exposing the specimen for 5 min at temperatures rising in 50 K increments from 373 to 873 K. The composition of the specimen was determined using inductively coupled plasma atomic emission spectrometry. The Rietveld method<sup>4</sup> was used to determine the precise structure, and RIETAN (Ref. 5) was used as the analytical program. Data in the range of angles between  $6.0^\circ$  and  $26.5^\circ$  were used for the analyses.

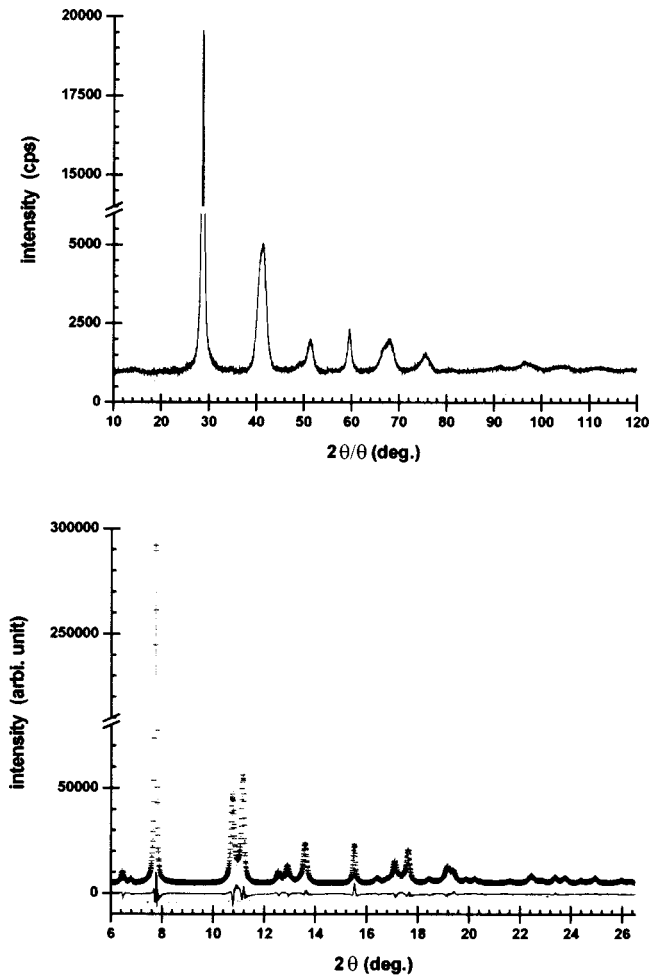


FIG. 1. X-ray-diffraction pattern of a  $\text{Ag}_{3.4}\text{In}_{3.7}\text{Sb}_{76.4}\text{Te}_{16.5}$  quadruple compound taken at room temperature using a conventional powder diffractometer with a curved graphite counter monochromator and a rotating Cu anode (upper figure). Observed (+) and calculated (gray line) synchrotron diffraction patterns are shown for  $\text{Ag}_{3.4}\text{In}_{3.7}\text{Sb}_{76.4}\text{Te}_{16.5}$  at room temperature (300 K). A difference curve (observed—calculated) appears at the bottom (lower figure).

### III. RESULTS

The composition of the compound was  $\text{Ag}_{3.4}\text{In}_{3.7}\text{Sb}_{76.4}\text{Te}_{16.5}$  and the wavelength of the irradiated beam was 0.4234 Å, short enough to make no absorption correction. As seen in Fig. 1, the diffraction pattern obtained shows substantially better peak separation than in the laboratory, and a good signal-to-noise ratio up to the neighborhood of  $2\theta = 30^\circ$ . This corresponds to the data collected in the range of  $2\theta = 140^\circ$  by  $\text{CuK}\alpha$  radiation.

The result of a search-match analysis revealed the diffraction pattern to be almost identical to that of As, Sb, or Bi crystal with an A7 structure.<sup>6</sup> The A7 structure is shown in Fig. 2. The atoms are in  $6(c)$  with  $z = 0.233\text{--}0.237$  (Ref. 7) of  $R\bar{3}m$ .<sup>8</sup> Therefore, the assumption was made for the compound of  $\text{Ag}_{3.4}\text{In}_{3.7}\text{Sb}_{76.4}\text{Te}_{16.5}$  that its space group is  $R\bar{3}m$  and Ag, In, Sb, and Te randomly occupy the  $6(c)$  site. The results of the Rietveld analyses for 81 and 300 K are shown in Fig. 1 and Table I. Anisotropic temperature factors were

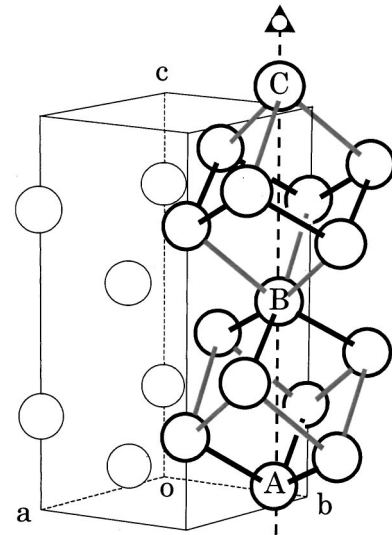


FIG. 2. A7-type crystal structure is shown schematically in perspective. The unit cell is shown by means of the hexagonal lattice. Open circles show atomic positions. Interatomic bonds, illustrated with thick black and gray lines, show the two kinds of basic cells distorted in the direction parallel to the threefold rotation-inversion axis. Atoms labeled A, B, and C exist on the same axis. The black and gray lines represent the shorter ( $r_s$ ) and longer ( $r_l$ ) bonds, respectively.

applied. As seen in Fig. 1, the observed and the calculated patterns show good agreement with each other.

Changes in diffraction lines with increasing temperature are shown in Fig. 3. The single-phase A7 structure continues up to 600 K, but peaks for  $\text{Sb}_2\text{O}_3$  ( $Fd\bar{3}m$ ,  $a = 11.152$  Å at  $26^\circ\text{C}$ ) (Ref. 9) appear at 623 K along with those indicating

TABLE I. Refined structural parameters for  $\text{Ag}_{3.4}\text{In}_{3.7}\text{Sb}_{76.4}\text{Te}_{16.5}$  at several typical temperatures. The space group  $R\bar{3}m$  is applied to all. The standard deviations are shown in parentheses.  $R_e$  means  $R_{wp}$  expected.

Temp (K)	81	300	723	823
$a$ (Å)	4.3470(2)	4.3553(3)	4.3696(3)	4.3747(2)
$c$ (Å)	11.2415(8)	11.2760(8)	11.5759(11)	5.8087(4)
site	$6(c)$	$6(c)$	$6(c)$	$3(a)$
$x$	0	0	0	0
$y$	0	0	0	0
$z$	0.2354(4)	0.2357(5)	0.2449(11)	0
$U_{11}$ (Å <sup>2</sup> )	0.007(3)	0.015(35)	0.034(3)	0.040(5)
$U_{22}$ (Å <sup>2</sup> )	$U_{11}$	$U_{11}$	$U_{11}$	$U_{11}$
$U_{33}$ (Å <sup>2</sup> )	0.022(5)	0.035(5)	0.092(6)	0.070(8)
$U_{12}$ (Å <sup>2</sup> )	$U_{11}/2$	$U_{11}/2$	$U_{11}/2$	$U_{11}/2$
$U_{23}$ (Å <sup>2</sup> )	0	0	0	0
$U_{13}$ (Å <sup>2</sup> )	0	0	0	0
$R_{wp}$ (%)	6.77	5.11	6.40	7.08
$R_e$ (%)	0.94	1.08	2.52	2.54
$R_p$ (%)	4.99	3.56	4.14	4.97
$R_I$ (%)	0.66	0.53	2.51	2.01
$R_F$ (%)	0.41	0.34	1.46	1.16

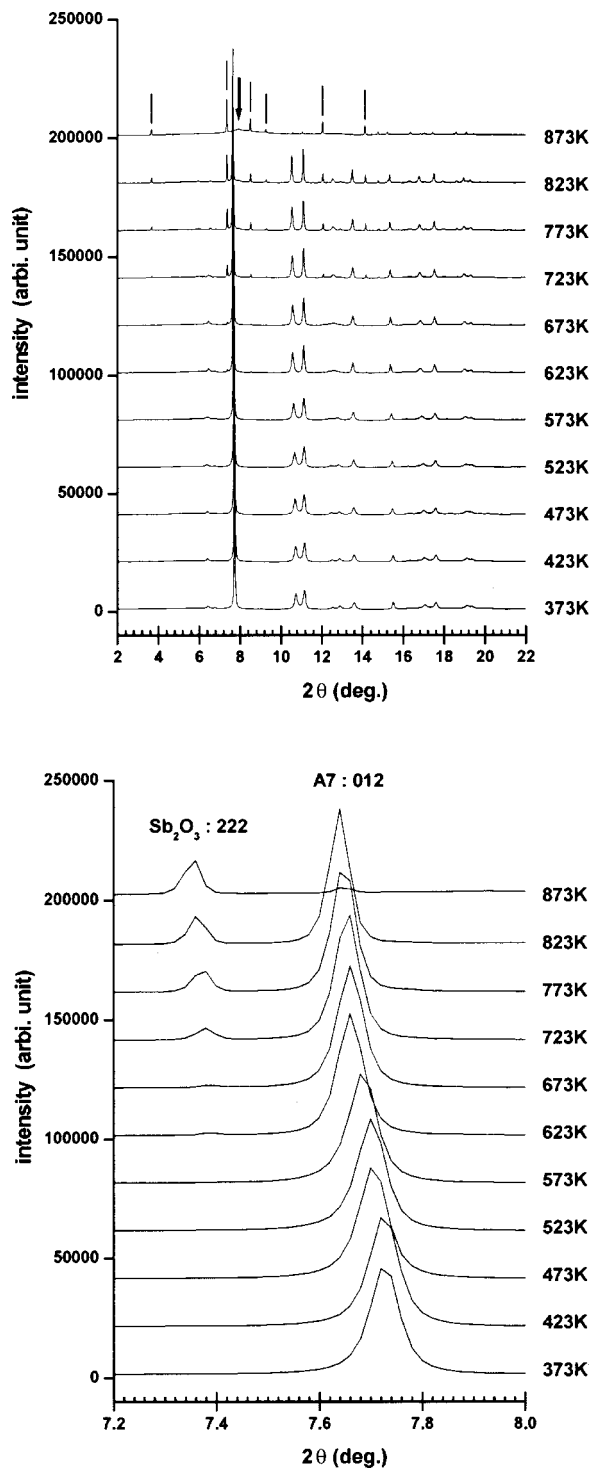


FIG. 3. X-ray-diffraction patterns of  $\text{Ag}_{3.4}\text{In}_{3.7}\text{Sb}_{76.4}\text{Te}_{16.5}$  are shown in order of temperature at intervals of 50 K. Vertical lines indicate positions of strong peaks for  $\text{Sb}_2\text{O}_3$ . The arrow in the figure identifies the halo peak for the amorphous phase. The lower figure is magnified between  $7.2^\circ$  and  $8.0^\circ$  in  $2\theta$ .

an A7 structure. It is presumed that Sb is selectively oxidized at this point. While coexisting with the A7 structure, the proportion of  $\text{Sb}_2\text{O}_3$  increases with rising temperature. The amount of generated  $\text{Sb}_2\text{O}_3$  was analyzed using the Rietveld method (Table II). The A7 structure continues to exist in

crystalline form at least up to 823 K; however, all the peaks indicating the A7 structure disappear at 873 K and a halo pattern appears instead, indicating probable transition to an amorphous phase. Rietveld analyses were made of all the high-temperature measurements using the data for  $6.0^\circ$ – $26.5^\circ$  with a step width of  $0.02^\circ$ . In addition, at temperatures higher than 623 K, the analyses were made in the two-phase system of  $\text{Ag}_{3.4}\text{In}_{3.7}\text{Sb}_{76.4}\text{Te}_{16.5}$  and  $\text{Sb}_2\text{O}_3$ . The composition of  $\text{Ag}_{3.4}\text{In}_{3.7}\text{Sb}_{76.4}\text{Te}_{16.5}$  was assumed to remain unchanged regardless of the amount of  $\text{Sb}_2\text{O}_3$ . The Rietveld result for 723 K is shown in Table I. Final  $R$  factors for  $\text{Sb}_2\text{O}_3$  are  $R_I=2.35\%$  and  $R_F=1.66\%$ . Changes with temperature in the lattice constants, in the unit-cell volume, and in the atomic coordinate ( $z$ ) are shown in Figs. 4, 5, and 6, respectively. The errors that are statistically predicted by the Rietveld method are also shown in the figures. Those for the lattice constant and the unit-cell volume, however, are smaller than the marks,  $\blacksquare$ ,  $\circ$ , and  $\bullet$ .

Based on the changes with temperature of the  $a$ - and  $c$ -axis lengths and of the unit-cell volume shown in Figs. 4 and 5, coefficients of linear expansion in the  $a$  and  $c$  axes and of cubical expansion were calculated. They were approximately  $0.86 \times 10^{-5}$ ,  $5.40 \times 10^{-5}$ , and  $9.16 \times 10^{-5}/\text{K}$ , respectively. On the other hand, the coefficient of linear expansion of Sb is known to be  $0.80 \times 10^{-5}$  (perpendicular to the  $c$  axis) and  $1.72 \times 10^{-5}$  (parallel to the  $c$  axis).<sup>10</sup>  $\text{Ag}_{3.4}\text{In}_{3.7}\text{Sb}_{76.4}\text{Te}_{16.5}$  showed a particularly large value for the coefficient of linear expansion parallel to the  $c$  axis compared with Sb. The calculated density of this quadruple compound was  $6.56 \text{ g/cm}^3$  (300 K). On the other hand, that of Sb is  $6.69 \text{ g/cm}^3$  (293 K).<sup>10</sup>

#### IV. DISCUSSIONS

The compound  $\text{Ag}_{3.4}\text{In}_{3.7}\text{Sb}_{76.4}\text{Te}_{16.5}$  has an A7 structure in the low-temperature phase. Its crystal structure shows little change up to 600 K, but above this temperature the atomic position changes significantly with increasing temperature. At around 780 K, a phase transition into another crystal structure occurs. Further details are discussed below.

##### A. Structure of the low-temperature phase

Although  $\text{Ag}_{3.4}\text{In}_{3.7}\text{Sb}_{76.4}\text{Te}_{16.5}$  is a quadruple compound, our results revealed that all atoms can randomly occupy each of the atomic positions in the A7 structure, at least at 81 K and above. This structure can be regarded as a disordered version of the A7 type. Further issues that need to be examined are whether this disordered structure exists as a supercooled state and whether an ordered structure exists. As shown in Fig. 2, the A7 structure comprises two kinds of hexahedrons linked to form a geometric unit. One is compressed along the threefold rotation-inversion axis and the other is expanded. The whole crystal can be obtained by repetitions of the parallel translations of a set of these cells. If these cells were the same sized and shaped rhombohedra or cubes, which actually occurs when the atomic position  $z$  is  $\frac{1}{4}$ , each atom in the crystal would have six nearest neighbors at equal distances. But in the A7 structure, there are three

TABLE II. The amounts of  $\text{Sb}_2\text{O}_3$ , which is formed above approximately 600 K, are listed in order of measurement temperature. In addition, the intensities of some superlattice reflections and (110) fundamental reflection are tabulated. The unit of intensity is arbitrary.  $2\theta$  angles of each reflection at 300 and 733 K are shown in the lower part of the Table.

$T$ (K)	$\text{Sb}_2\text{O}_3$ (wt. %)	$I_{\text{obs}}^S(003)$	$I_{\text{obs}}^S(101)$	$I_{\text{obs}}^S(015)$	$I_{\text{obs}}^S(113)$	$I_{\text{obs}}^F(110)$
81	—	3350	1048	5055	3506	35 194
300	—	3483	1029	4754	3185	34 187
373	—	3451	1071	4785	3284	35 100
423	—	3830	1204	5082	3484	34 883
473	—	3846	1187	5018	3424	35 145
523	—	3291	1008	4495	3031	33 924
573	—	3550	1168	4508	3184	36 128
623	1.2	2105	690	2565	1734	34 529
673	1.2	2131	703	2607	1766	34 367
723	6.0	742	246	855	583	33 053
773	10.8	27	9	28	20	32 121
823	13.1	0	0	0	0	29 943

$T$ (K)	$2\theta$ (003)	$2\theta$ (101)	$2\theta$ (015)	$2\theta$ (113)	$2\theta$ (110)
300	6.46°	6.79°	12.56°	12.90°	11.16°
773	6.28°	6.74°	12.29°	12.77°	11.11°

shorter interatomic distances ( $r_s$ ) and three longer distances ( $r_l$ ) between the central atom and its six neighbors. The  $r_s/r_l$  of As, Sb, and Bi approach 1 in that order. In Table III we show the crystallographic data relevant to As, Sb, and Bi,<sup>11</sup> and  $\text{Ag}_{3.4}\text{In}_{3.7}\text{Sb}_{76.4}\text{Te}_{16.5}$ . The  $r_s$  bond is thought to be covalent.<sup>11</sup> At room temperature, their bond angles are slightly greater than  $90^\circ$ .  $\text{Ag}_{3.4}\text{In}_{3.7}\text{Sb}_{76.4}\text{Te}_{16.5}$  has both its  $r_s/r_l$  and bond angle between those of Sb and Bi at room temperature.

### B. Temperature dependency of the structure

As shown in Fig. 6,  $z$  in 6(c) remains at 0.235–0.236 up to around 600 K, but rapidly increases as the temperature continues to rise, reaching almost  $\frac{1}{4}$  near 780 K. The changes

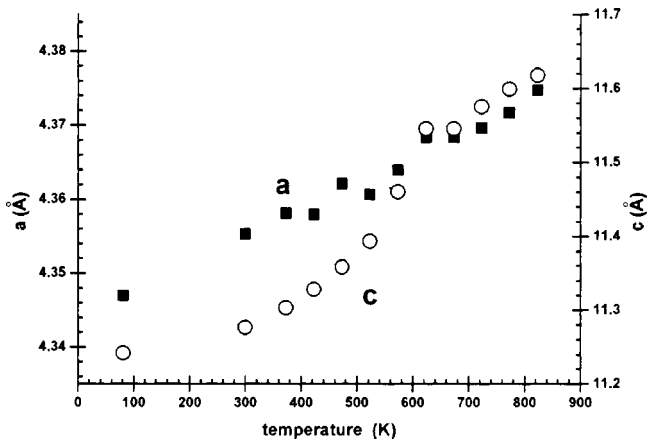


FIG. 4. Temperature dependence of the  $a$  and  $c$  axes of  $\text{Ag}_{3.4}\text{In}_{3.7}\text{Sb}_{76.4}\text{Te}_{16.5}$ . Filled squares and open circles represent  $a$  and  $c$ , respectively.

in the  $r_s/r_l$  ratio and the bond angle as a function of temperature are shown in Fig. 7. In connection with the  $z$  shift,  $r_s/r_l$  maintains approximately 0.88 up to around 600 K but rapidly increases above the temperature, closely approaching 1 near 780 K. On the other hand, the bond angle shifts from  $94.0^\circ$ – $95.0^\circ$  to  $86.8^\circ$  (at 823 K). Extrapolating from the changes in  $r_s/r_l$  with temperature at temperatures above 780 K,  $r_s/r_l$  is likely to become larger than 1. However,  $r_s/r_l$  is still 1 at 823 K.

Figure 8 shows the temperature factor analyzed on the assumption that the thermal vibration of the atoms is isotropic. The factor changes in an approximately exponential function with linearly increasing temperature, and particularly rapidly from around 600 K. At this temperature,  $\text{Sb}_2\text{O}_3$  starts to form, with its volume rapidly increasing with tem-

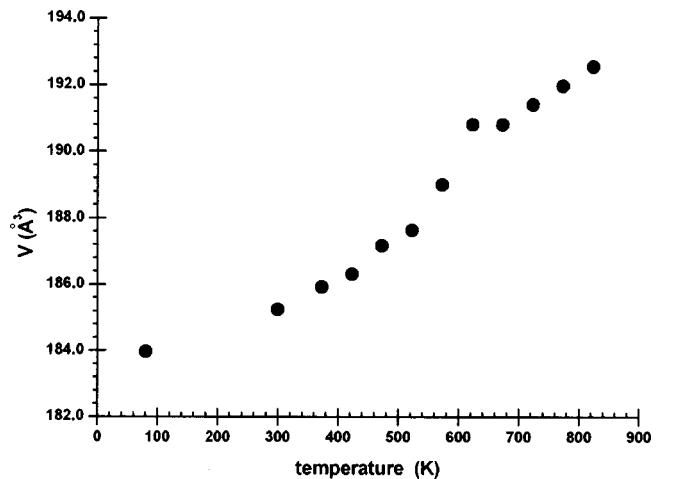


FIG. 5. Temperature dependence of the unit cell volume of  $\text{Ag}_{3.4}\text{In}_{3.7}\text{Sb}_{76.4}\text{Te}_{16.5}$ .

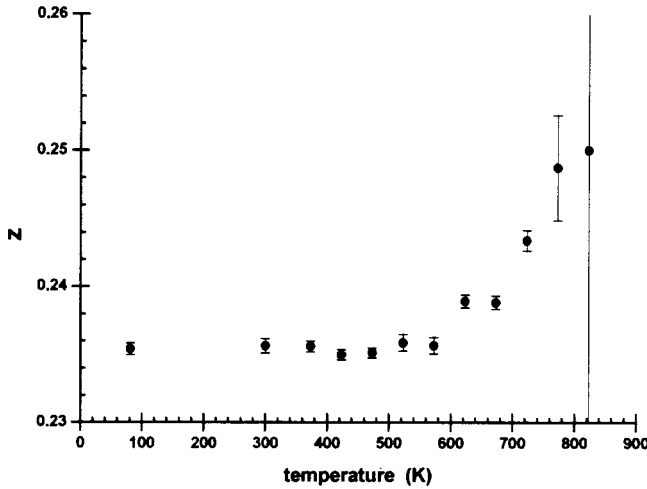


FIG. 6. Temperature dependence of  $z$  in the 6( $c$ ) site of  $\text{Ag}_{3.4}\text{In}_{3.7}\text{Sb}_{76.4}\text{Te}_{16.5}$ . The error of  $z$  at 823 K is 0.098. However, in practice,  $z$  is fixed at  $1/4$  by the phase change, which makes the error 0.

perature. At 823 K, just before transforming into an amorphous state, mean atomic displacement due to thermal vibration is approximately 0.28 Å, around 10% of the closest interatomic distance. Here, we used  $B_0 = 8\sigma^2\pi^2$  for the relationship between the isotropic temperature factor  $B_0$  and the mean atomic displacement  $\sigma$ .

We assumed the composition of the A7 structure remained unchanged as  $\text{Ag}_{3.4}\text{In}_{3.7}\text{Sb}_{76.4}\text{Te}_{16.5}$  regardless of the amount of  $\text{Sb}_2\text{O}_3$  generated. However, for example at 773 K, it is presumed that around 10.8 wt% of  $\text{Sb}_2\text{O}_3$  is formed, as shown in Table II. When the Sb in  $\text{Ag}_{3.4}\text{In}_{3.7}\text{Sb}_{76.4}\text{Te}_{16.5}$  is selectively oxidized, the composition of the quadruple phase is presumed to change to  $\text{Ag}_{3.8}\text{In}_{4.1}\text{Sb}_{73.7}\text{Te}_{18.4}$ . A Rietveld analysis was made of the two-phase system of  $\text{Ag}_{3.8}\text{In}_{4.1}\text{Sb}_{73.7}\text{Te}_{18.4}$  and  $\text{Sb}_2\text{O}_3$  using the diffraction data taken at 773 K. The crystallographic data obtained, however, are almost same as the results of the analysis made in the two-phase system of  $\text{Ag}_{3.4}\text{In}_{3.7}\text{Sb}_{76.4}\text{Te}_{16.5}$  and  $\text{Sb}_2\text{O}_3$ .

### C. Structure of the high-temperature phase

As already mentioned, when  $z = 1/4$  in the A7 structure, each of the two hexahedrons in Fig. 2 forms a single completely congruent rhombohedron, which means the whole crystal can be obtained by iterative parallel translations of the rhombohedron. This polyhedron thus becomes a unit cell, in which only one atom exists, and in the hexagonal notation, the length of the  $c$  axis becomes half of the A7 structure.

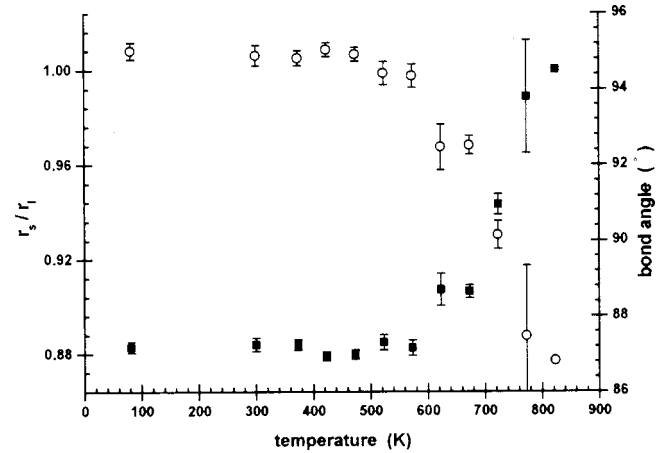


FIG. 7. Temperature dependence of  $r_s/r_l$  and bond angle. Filled squares and open circles represent  $r_s/r_l$  and bond angles, respectively.

This structure can be approximately described with any space group of  $R3$ ,  $R\bar{3}$ ,  $R32$ ,  $R3m$ , and  $R\bar{3}m$ . As discussed in Sec. IV D, however, this structural transformation is predicted to be the second order phase transition. Therefore, it is logical to presume that the space group in the high temperature phase is  $R32$  or  $R3m$ , which is the subgroup of the symmetry of  $R\bar{3}m$ .<sup>12</sup> We discuss the validity of this assumption below.

We refined the structural parameters of the high-temperature phase at 823 K with anisotropic temperature factors in the space group  $R\bar{3}m$  using the Rietveld method. The results are shown in Table I. Then using the  $F_o$  estimated and  $F_c$  determined by the analysis, we carried out a difference synthesis in the space group  $R3m$ . The difference Fourier map is shown in Fig. 9. No center of symmetry exists at the center of the map. We refined the structural parameters of the low-temperature phase at 723 K in a similar fashion, and carried out a difference synthesis. As can be seen in the figure, a center of symmetry clearly exists at the center of the map. Also, in the difference Fourier maps made with the space group  $R32$ , the low-temperature phase, but not the high-temperature phase, shows a center of symmetry. Therefore, the space group of the high-temperature phase is considered to be  $R32$  or  $R3m$ . In short, no center of symmetry exists in the electron density distribution in the crystal in the high-temperature phase. To determine the correct space group,  $R32$  or  $R3m$ , further detailed analysis will be required.

TABLE III. Crystallographic data for As, Sb, Bi, and  $\text{Ag}_{3.4}\text{In}_{3.7}\text{Sb}_{76.4}\text{Te}_{16.5}$ , having an A7 structure at room temperature.

	$a$	$c$	$r_s$	$r_l$	$r_s/r_l$	Bond angle
As	3.760 Å	10.548 Å	2.506 Å	3.137 Å	0.80	97.2°
Sb	4.308 Å	11.274 Å	2.902 Å	3.362 Å	0.86	95.8°
Bi	4.546 Å	11.862 Å	3.110 Å	3.480 Å	0.89	93.9°
$\text{Ag}_{3.4}\text{In}_{3.7}\text{Sb}_{76.4}\text{Te}_{16.5}$	4.355 Å	11.276 Å	2.955 Å	3.343 Å	0.88	94.9°

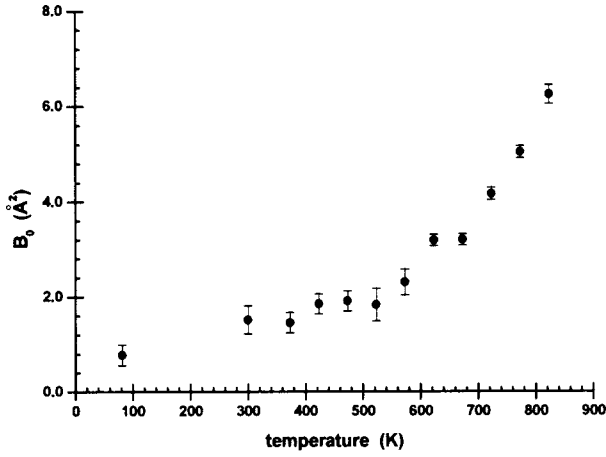


FIG. 8. The isotropic temperature factors are shown as functions of temperature.

#### D. Phase-transition properties

When atoms are only at  $0, 0, z$  in  $6(c)$  of  $R\bar{3}m$ , its structure factor  $F(hkl)$  can be written as

$$F(hkl) = f \cos(2\pi lz) \left\{ 1 + \exp \left[ 2\pi i \left( \frac{2}{3}h + \frac{1}{3}k + \frac{1}{3}l \right) \right] \right. \\ \left. + \exp \left[ 2\pi i \left( \frac{1}{3}h + \frac{2}{3}k + \frac{2}{3}l \right) \right] \right\}, \quad (1)$$

where  $f$  is the atomic scattering factor. Regarding the term of  $\cos(2\pi lz)$ , it is understood that all of  $F(hkl)$  with an odd-numbered  $l$  is 0, when  $z$  is  $\frac{1}{4}$  (or  $\frac{3}{4}$ ). Equation (1) indicates that  $hkl$  with an even-numbered  $l$  can be considered to be the fundamental reflection and  $hkl$  with an odd  $l$  to be the superlattice reflection. Notably, the  $F$  of the  $hk0$  fundamental reflection is constant regardless of  $z$ . As shown in Fig. 10, the peak of the 015 superlattice reflection gradually diminishes with increased temperature, with its intensity falling to zero at around 780 K. In Table II we show the observed intensities of some superlattice reflections  $I_{\text{obs}}^S(003)$ ,  $I_{\text{obs}}^S(101)$ ,  $I_{\text{obs}}^S(015)$ , and  $I_{\text{obs}}^S(113)$ ; and the fundamental reflection,  $I_{\text{obs}}^F(110)$  vs measurement temperatures. All the intensities of the superlattice reflections are 0 at temperatures above 780 K. Therefore, it is concluded that the length of the  $c$  axis of the unit cell can be shortened by half, and that  $z$  is locked at  $\frac{1}{4}$ .

As already mentioned, the crystal structure, i.e.  $r_s/r_l$ , bond angle, etc., changes continuously with temperature. Thus this structure transformation is presumed to be a second-order phase transition. From many experiments on various substances investigating this type of phase transition, it is known that when approaching the critical temperature  $T_c$ , physical properties generally change as  $|T - T_c|^\beta$ .<sup>13</sup> The exponent  $\beta$  is usually termed the critical index. Fig. 11 shows  $1/4 - z$  vs temperature. The curve in this figure was made using the least-squares method over the temperature range of 523–773 K.  $1/4 - z$  varies in close proportionally to

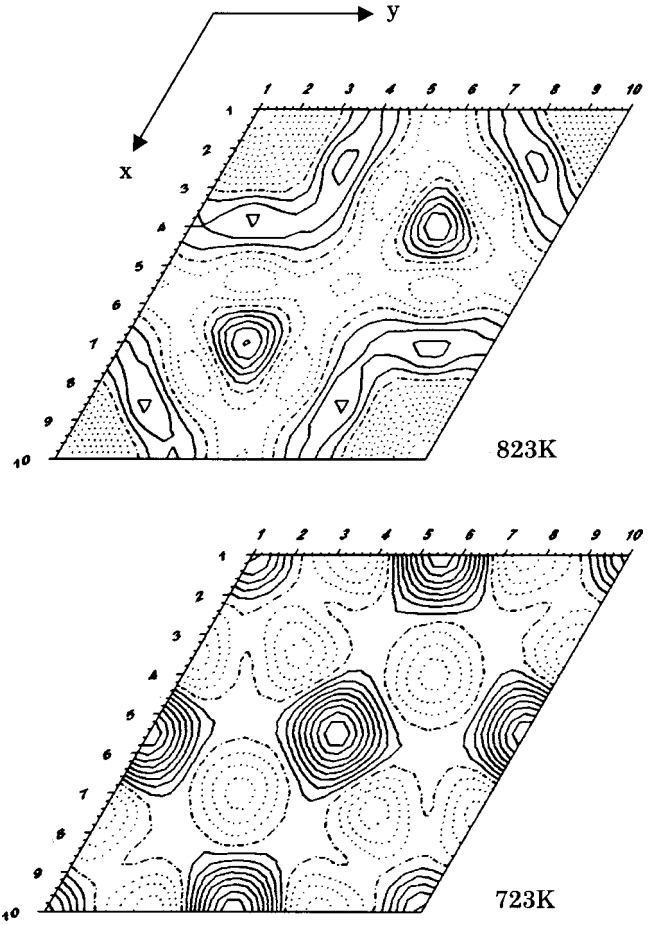


FIG. 9. Difference Fourier maps in the  $c$  plane ( $z=0$ ) of the hexagonal unit cell. The contours are drawn at  $0.05e \text{ \AA}^{-3}$ . Negative regions are represented by dashed lines.

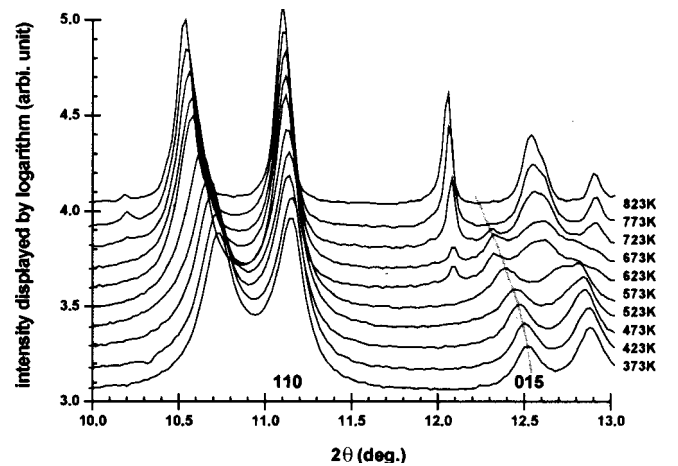


FIG. 10. X-ray-diffraction patterns of  $\text{Ag}_{3.4}\text{In}_{3.7}\text{Sb}_{76.4}\text{Te}_{16.5}$  from  $2\theta = 10^\circ - 13^\circ$  are shown in order of temperature at intervals of 50 K. Peak positions shift toward the low angle side with increasing temperature owing to the thermal expansion of the lattice. The (015) peak gradually diminishes with increased temperature, but the intensity of the (110) peak remains virtually unchanged.

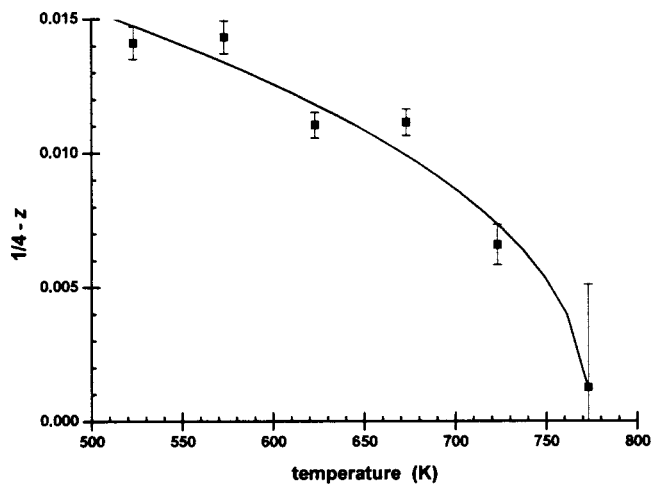


FIG. 11.  $1/4-z$  is shown as a function of temperature. The solid line was obtained by fitting  $(T-T_c)^\beta$  to  $1/4-z$  using the least squares method in the range from 523 to 773 K.

$(T_c - T)^\beta$ .  $T_c$  is  $774 \pm 5$  K, and  $\beta$  is  $0.43 \pm 0.10$ . Similarly, it has been confirmed that  $I_{\text{obs}}^S/I_{\text{obs}}^F$  are proportional to  $(T_c - T)^\beta$  as well.

When a crystal structure changes as the result of a second-order phase transition, in most cases the high-temperature phase shows a higher symmetry than the low-temperature phase. It is known, however, that sometimes the opposite is the case. Potassium sodium tartrate,  $\text{NaK}(\text{C}_4\text{H}_4\text{O}_6) \cdot 4\text{H}_2\text{O}$ , has two second-order phase transition points at  $-18$  and  $24$  °C. Between these two transition temperatures, this crystal has a monoclinic structure. Outside this range, it forms an orthorhombic structure. At  $-18$  °C, the symmetry falls with increased temperature.<sup>14</sup>

## V. CONCLUSIONS

By using well-monochromated and -paralleled synchrotron radiation and a large Debye-Scherrer camera, diffraction patterns with good peak separation and a good signal-to-noise ratio were obtained. Rietveld analyses were then carried out successfully. The compound of  $\text{Ag}_{3.4}\text{In}_{3.7}\text{Sb}_{76.4}\text{Te}_{16.5}$  has an  $A7$  structure with its four constituent atoms randomly occupying the  $6(c)$  sites of  $R\bar{3}m$ . The crystal lattice thermally expands almost linearly with temperature between 81 and 823 K. The linear coefficient of expansion along the  $c$ -axis direction is substantially larger than that of Sb. The crystal structure shows little change between 81 K and around 600 K. At temperatures above 600 K, though, while maintaining its  $A7$  structure, the thermal vibration of atoms, the volume, the  $r_s/r_l$  ratio, the bond angle, etc. change markedly with temperature. Oxidation also becomes marked over 600 K. As the temperature increases, the crystal is transformed into a rhombohedral structure containing one atom in each unit cell; in hexagonal notation, three atoms are contained in a unit cell. This structure transformation is presumed to be a second-order phase transition that takes place at around 780 K. The highest temperature at which the compound of  $\text{Ag}_{3.4}\text{In}_{3.7}\text{Sb}_{76.4}\text{Te}_{16.5}$  can maintain its crystalline state is around 850 K. At temperatures higher than 850 K, it degenerates into an amorphous state.

## ACKNOWLEDGMENTS

The authors would like to express their appreciation to K. Katoh, Dr. E. Nishibori, Dr. Y. Kubota, Dr. M. Takata, and Dr. M. Sakata for their great assistance in the experiments at BL02B2 and their advice on structural analyses. They also wish to thank Dr. J. Harada of the X-Ray Research Laboratory at Rigaku Corporation for his valuable suggestions concerning this study.

\*Email address: matunaga@mtr.mei.co.jp

<sup>1</sup>H. Iwasaki, Y. Ide, M. Harigaya, Y. Kageyama, and I. Fujimura, *Jpn. J. Appl. Phys.* **25**, 1992 (1991).

<sup>2</sup>M. Takata and M. Yamakata, *SPring-8 Information* **5**, 88 (2000).

<sup>3</sup>M. Sakata, M. Takata, and E. Nishibori, *SPring-8 Information* **5**, 194 (2000).

<sup>4</sup>H. M. Rietveld, *J. Appl. Crystallogr.* **2**, 65 (1969).

<sup>5</sup>F. Izumi, *Nihon-Kesshōgaku-kaishi* **27**, 23 (1985) (in Japanese).

<sup>6</sup>G. L. Clark, *Applied X-Rays* (McGraw-Hill, New York, 1955).

<sup>7</sup>R. W. G. Wyckoff, *Crystal Structures* (Interscience, New York, 1963), Vol. 1.

<sup>8</sup>*International Tables for Crystallography*, edited by T. Hahn (Kluwer, Dordrecht, 1995), Vol. A.

<sup>9</sup>R. W. G. Wyckoff, *Crystal Structures* (Krieger, Malabar, FL, 1986).

<sup>10</sup>*Ri-Kagaku-Jiten*, edited by R. Kubo, S. Nagakura, H. Iguchi, and H. Ezawa (Iwanami, Tokyo, 1987) (in Japanese).

<sup>11</sup>R. Kiriya and H. Kiriya, *Structural Inorganic Chemistry* (Kyoritsu, Tokyo, 1979) (in Japanese).

<sup>12</sup>B. K. Vainshtein, V. M. Fridkin and V. L. Indenbom, *Structure of Crystals* (Springer-Verlag, Berlin, 1995).

<sup>13</sup>H. Yukawa, M. Toda, and R. Kubo, *Statistical Physics* (Iwanami, Tokyo, 1978) (in Japanese).

<sup>14</sup>L. D. Landau, A. I. Akhiezer, and E. M. Lifshits, *General Physics* (Pergamon, Oxford, 1967).